THERMAL INSULATIVE ELASTOMERS FOR CLUSTERED LARGE LIQUID PROPELLANT ROCKET ENGINES

by

S. T. Peters

Rocketdyne
A Division of North American Aviation, Inc.
Canoga Park,
California

Presented at the

Seventh National SAMPE Symposium
El Segundo, California
20-22 May 1964

THERMAL INSULATIVE ELASTOMERS FOR CLUSTERED LARGE LIQUID PROPELLANT ROCKET ENGINES

By S. T. Peters
Rocketdyne, A Division of North American Aviation, Inc.

May 21, 1964

Abstract

22920

As thrust levels increase and as rocket engines fire for longer periods of time, the difficulties encountered in the protection of critical components from the effects of excessively high temperatures greatly increase. To protect these components a series of filled elastomeric composites have been evaluated. A brief discussion is presented of the problems of hot gas recirculation, radiation, and base plane heating with particular reference to large, clustered, liquid propellant rocket engines. The effect on components is discussed and an evaluation of a series of insulators based on filled elastomeric composites is presented. The evaluations are based on specialized thermal tests which were designed to simulate as far as possible, conditions during flight. The most promising of these elastomeric composites are compared to three alternative insulative systems, a filled, castable ceramic, a metal foil-silica fiber batting, and an asbestos-inconel wire mesh composite, in terms of weight, cost, and ease of fabrication and repair.*

*Work described in this material was performed under contract No. NASW-16 under the technical direction of George C. Marshall, Space Flight Center.

THERMAL INSULATIVE ELASTOMERS FOR CLUSTERED LARGE LIQUID PROPELLANT ROCKET ENGINES

The size of liquid propellant rocket engines has grown enormously in the past few years. In addition, these engines are now being clustered to develop even more power. F-1 engines, clustered in a group of five for the Saturn V Booster, will develop a total of 7,500,000 pounds of thrust. Associated with the increase in boost power is an increase in time of flight, as well as problems in protecting components from excessive temperatures.

The environment to which areas of the engine and its components will be subjected incorporates both radiant and convective heat flux. Both types of heat flux vary over the entire flight time. Figure 1 shows the calculated variation in radiant and convective heat flux at the surface of an insulated fluid control valve well away from the exhaust jet as a function of flight time. Since the emissivity of the exhaust plume is high (approximately 0.80), because of luminous carbon particles contained in it, gas temperature and surface temperature rise markedly toward the nozzle exit. The most stringent conditions are obtained at the exit of the extension skirt, where reinforcing bands (hatbands) must provide structural stability. An estimated temperature profile for the lowest of these bands shielded and unshielded is shown in Fig. 2.

Since the booster, during the latter portions of flight will operate above the bulk of the earth's atmosphere (above 40,000 feet), the exhaust gases will tend to blow back into the engine compartment. This recirculation of gases occurs at approximately 80 seconds of flight time (Fig. 3) at an altitude of 40,000 feet. At this altitude the pressure of the exhaust gases at the nozzle exit exceeds the ambient air pressure, and the gases are free to expand in all directions, including back into the missile boat-tail, resulting in gas

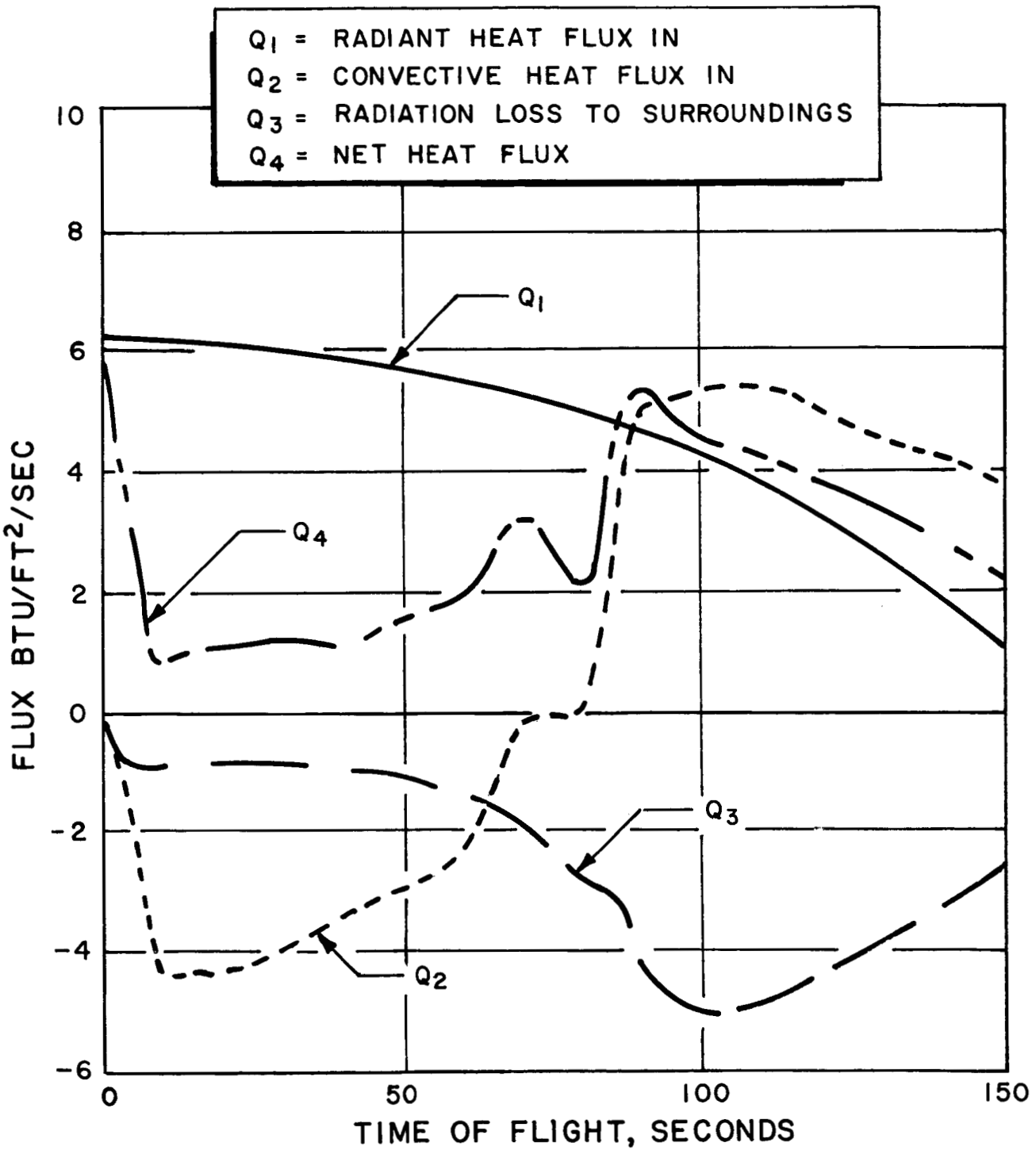

Figure 1. Expected Surface Heat Flux for a Bearing Coolant Control Valve Insulated with Foil Batting

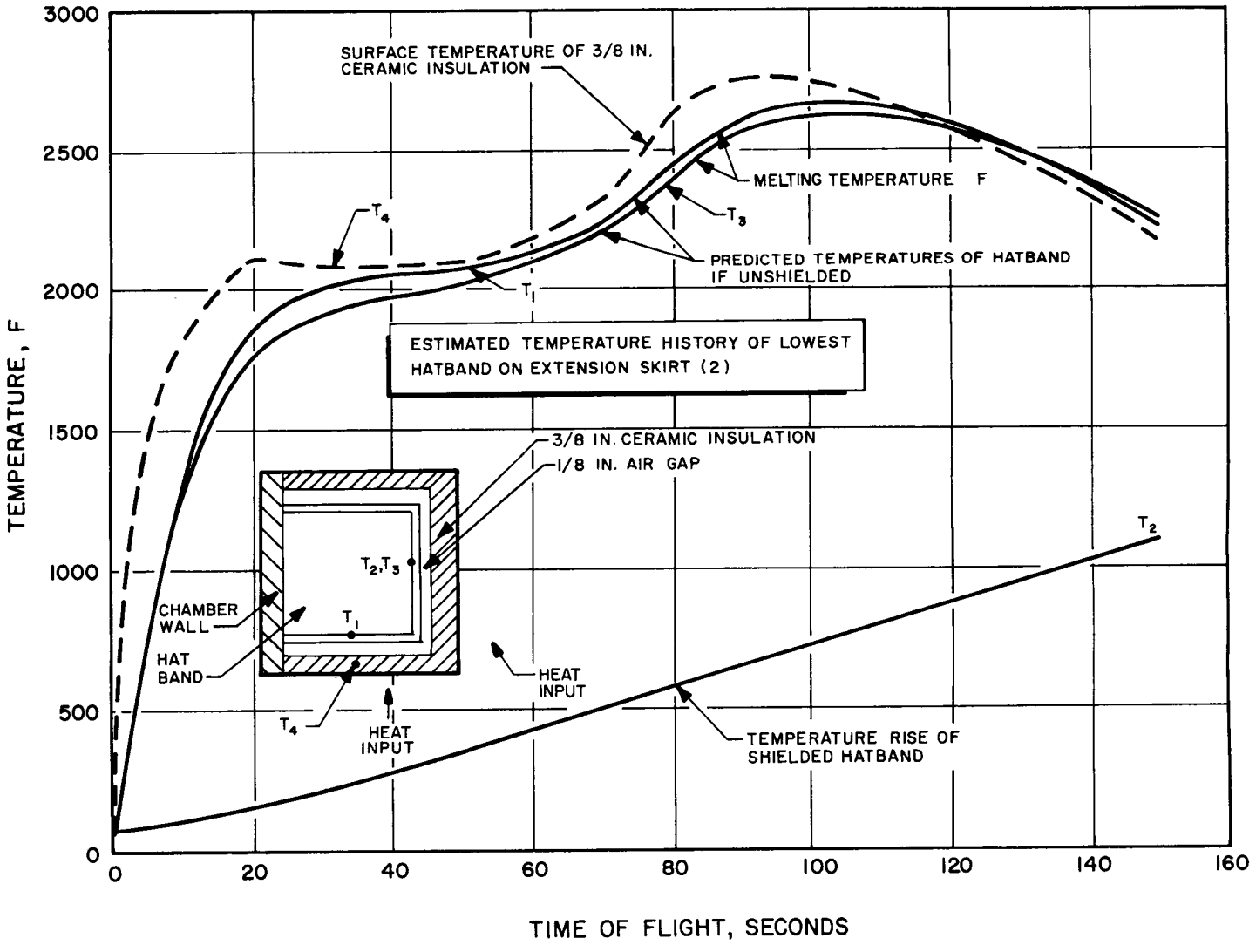

Figure 2. Estimated Temperature History of Lowest Hatband on Extension Skirt

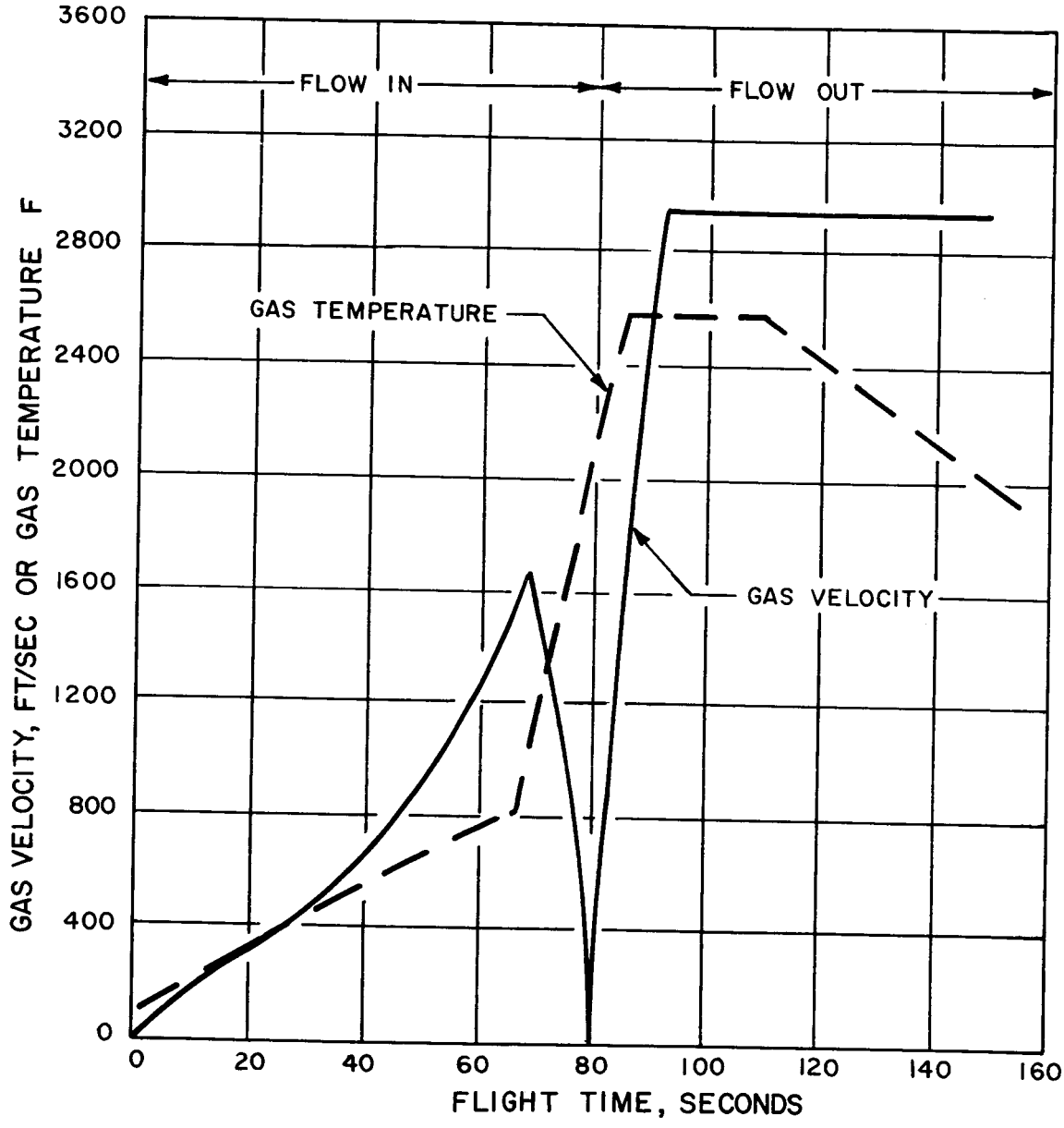

Figure 3. Estimated Velocity, Direction, and Temperature of Recirculating Hot Gas vs Flight Time

temperatures up to 2500 F around all components of the engine, even though they are quite distant (over 17 feet) from the nozzle exit plane. This recirculation causes the abrupt increase in convective flux after 80 seconds depicted in Fig. 1.

Radiant flux also varies over the flight time (Fig. 4). Although the level of radiation of the plume drops from 120 btu/ft^2 sec at ignition to about 10 btu/ft^2 sec at cutoff, the effect of this radiation is diminished less gradually. The carbon particles contained in the exhaust jet may deposit on the surface of components and increase their absorptivity.

All areas of the F-1 engine require some type of thermal protection. For most of the areas of the engine an inconel foil-high silica fiber batting seems adequate. This composite has a low density, 0.47 lbs/ft^2 at .375 thickness, has an upper temperature limit of 2000 F, and thermal conductivity on the order of .03 to 0.75 btu-ft/ft^2-hr-F. Because of extreme temperatures in some areas, however, the inconel foil-high silica fiber batting cannot be used and recourse must be made to one of three alternative systems. A castable ceramic has been developed which shows high temperature (above 1700 F) capability, good vibration resistance compared to other ceramics (when reinforced with wire mesh), and fairly low density. An asbestos wire-mesh composite has been considered as a means of lowering fabrication costs. These materials are compared to a typical high performance epoxy-polyamide, castable ablative in Table I.

Because drawbacks occur in any system of temperature control, ablatives have been considered only for areas in which there are marked advantages because of weight reduction, vibration resistance, or extreme ease of fabrication

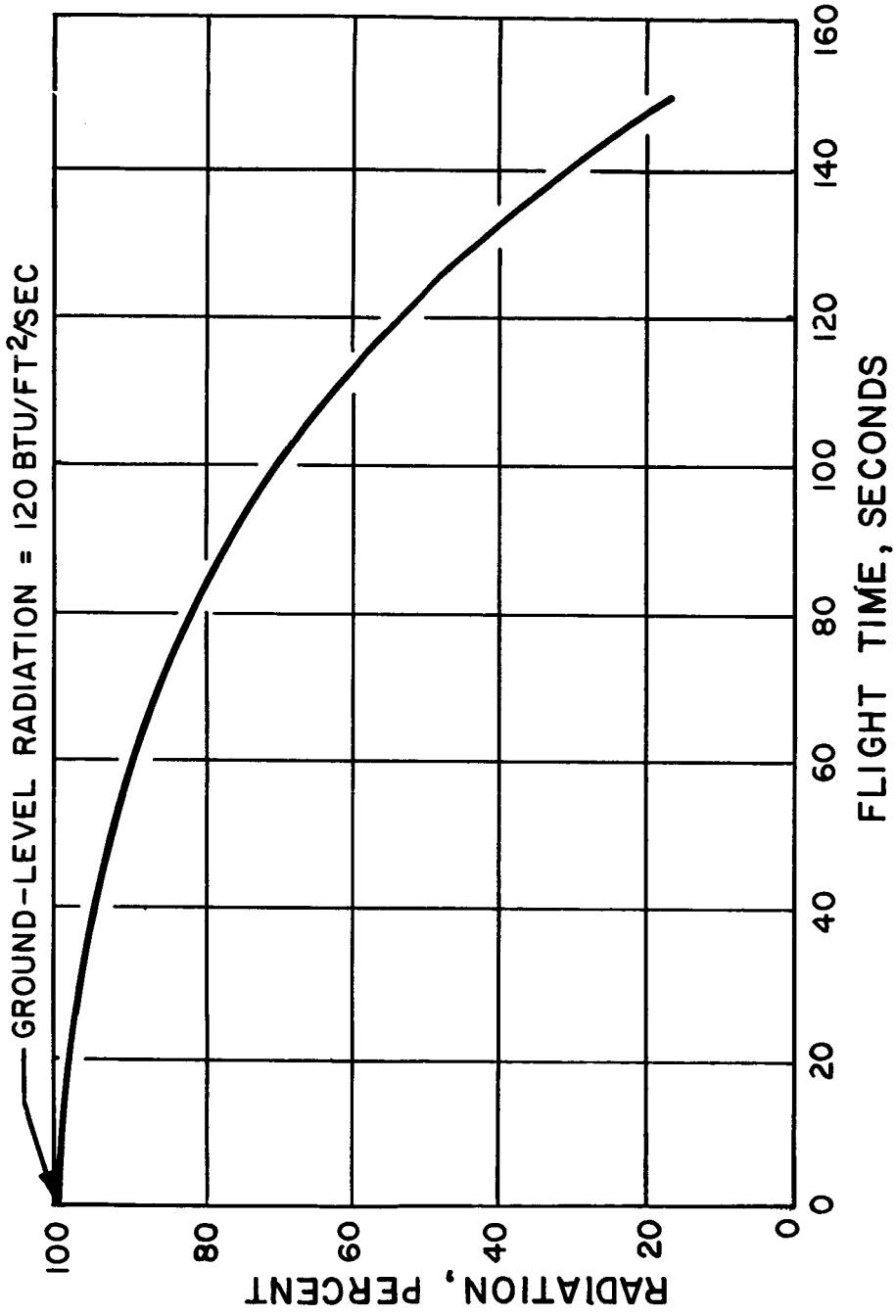

Figure 4. Percent of Radiation vs Flight Time

compared to the other systems. The areas which are particularly receptive to ablative cooling are the support members for, and the exterior of, the extension skirt, the turbine exhaust duct, and the hatbands surrounding the thrust chamber and the extension skirt, and the electrical harnesses. These areas (Fig. 5) are all fairly close to the nozzle exit plane and see high convective and radiant heat fluxes. The electrical harnesses, which must move during flight because of engine gimbaling, and must support their own weight while subjected to high "g" loadings, are particularly receptive to ablative elastomers.

The ablative materials considered have been mainly room or low temperature curing epoxies and silicones. Tested also were an air curing polyurethane, low temperature curing polyurethanes, and a flexible phenolic asbestos composition. The bulk of the materials tested are proprietary, but formulations were devised by Rocketdyne to test the effect of various fillers.

Rocketdyne has employed three tests for screening these materials. Each test was utilized with a definite application in mind, and all were modified to gain the greatest amount of reproducible data. Initially, it was decided to employ a standard test, reproducible industry-wide, for which there was a known, available, specification. This test, it was hoped, would make the data determined by Rocketdyne comparable to that disseminated by other agencies, thereby reducing the test load. The torch test described in BUWEPS OS9163 specification, however, seemed to reveal two drawbacks. The flux, measured to Rocketdyne's water cooled calorimeter was 194 btu/ft^2 sec; a much higher flux than that anticipated around components of the engine. Secondly, there was some question as to what the actual back-face temperature was,

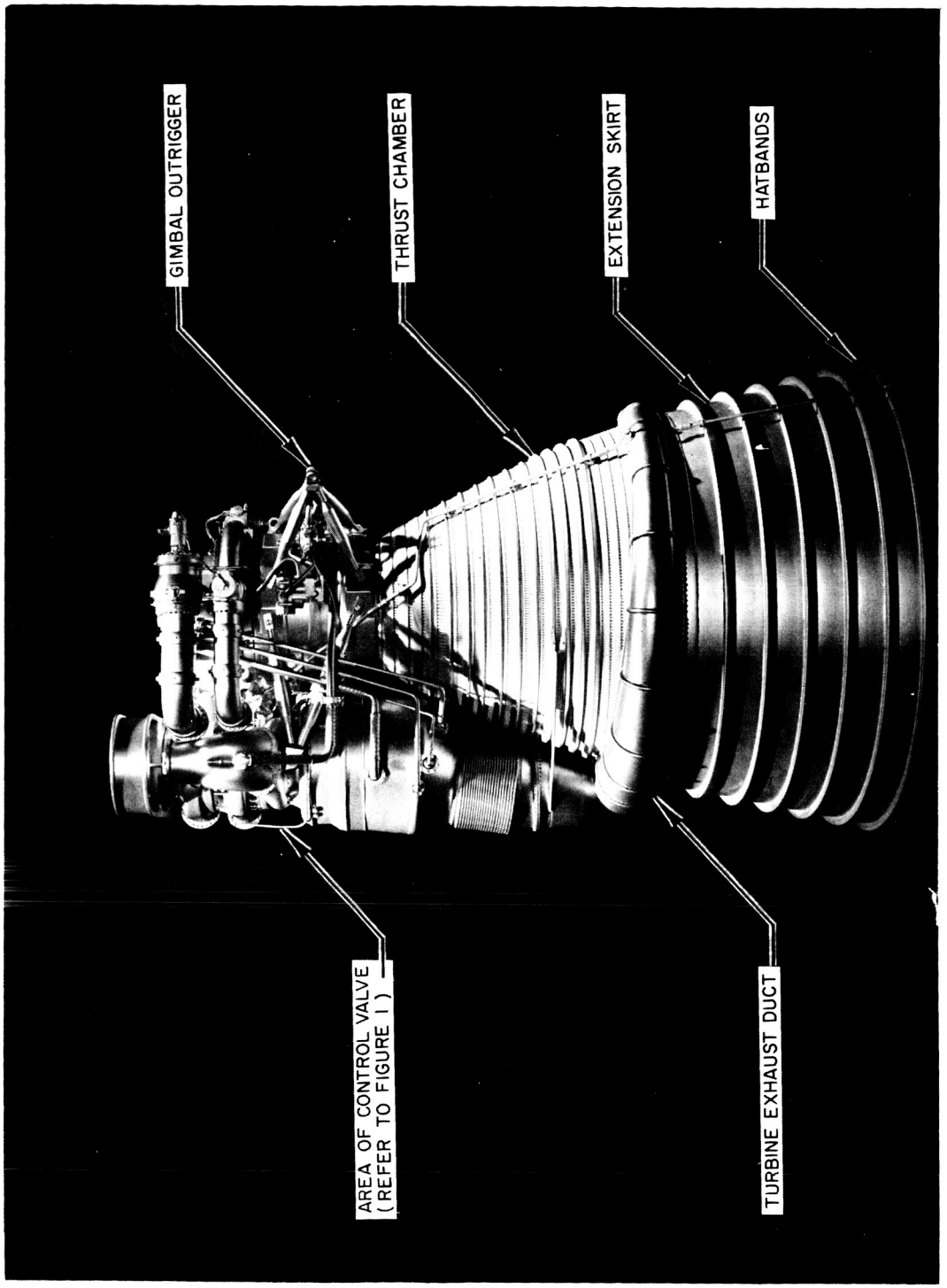

Figure 5. F-1 Engine

since there was an appreciable amount of heat absorbed by the steel backing plate and, consequently, a delay in the temperature rise. Figure 6 shows the results of a series of tests conducted by this method.

A natural gas-oxygen torch with a 4-inch extension was employed in the later tests. The specimens were molded to 2-inch diameter disks, of varying thicknesses and mounted vertically in transite guard sheets (Fig 7 shows a sample in position ready for test). In some cases a room temperature vulcanizing silicone adhesive was used to secure the sample in the guard sheet when an interference fit was not sufficient. A spring-loaded, platinum/platinum-10 percent rhodium thermocouple was placed at the back face of the specimen. The torch flowrate was adjusted to 120 cu ft/hr oxygen flow and 55 cu ft/hr gas flow, and the torch was brought to a distance (5-1/2 inches) from the specimen which would result in a flux of 50 btu/ft^2/hr of convective flux to a cold wall calorimeter. The sample was tested at this flux until failure, or until a significant rise in back-face temperature occurred. Failure was usually indicated by the sample disintegrating at the center under the slight load of the spring loaded thermocouple. Figure 8 shows the back-face temperature rise for a number of materials tested in this manner.

This test was also modified to simulate the actual changes in flux and temperature which an insulator might experience during flight. The available heat flux was varied over the test time period by changing the torch to specimen distance. The test setup is shown in Fig. 9, the heat flux range and front-face temperatures are shown in Fig. 10, and the results of these tests are shown in Fig. 11.

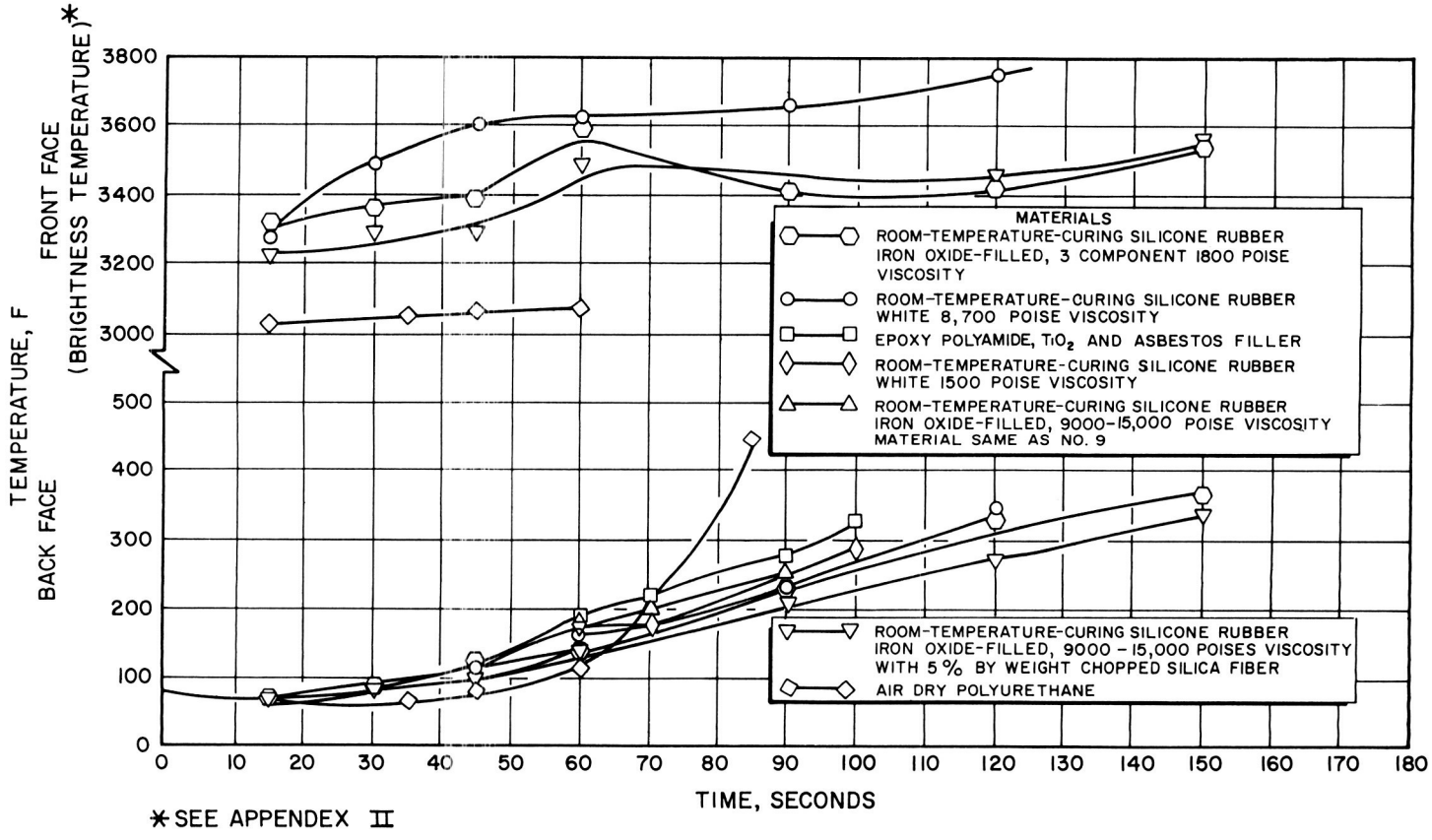

Figure 6. BUWEPS OS 9163 Torch Test Back-Face and Front-Face Temperatures vs Time

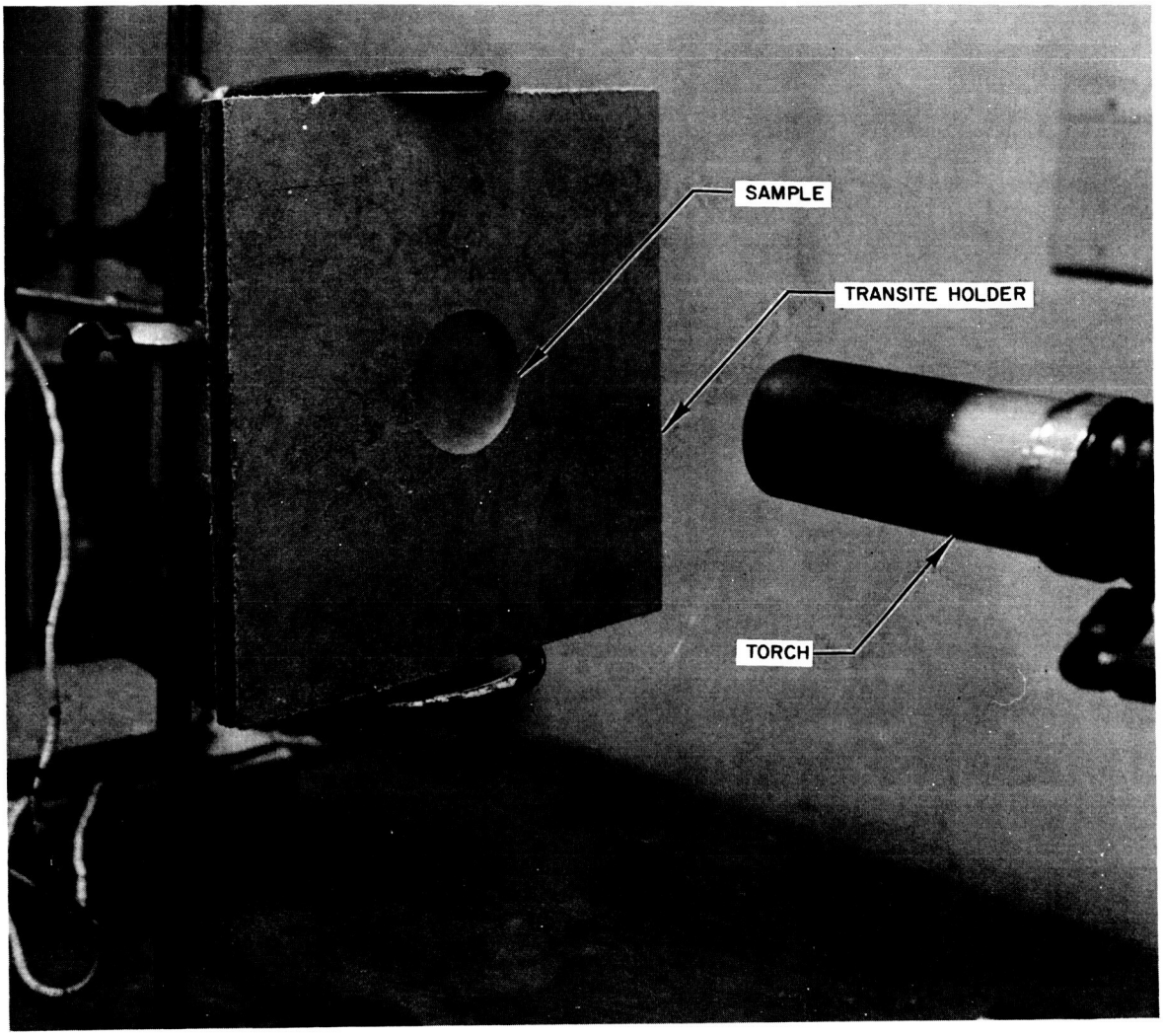

Figure 7. Natural Gas Oxygen Torch Test Constant 50 Btu/ft^2 sec Heat Flux Sample in Test Position

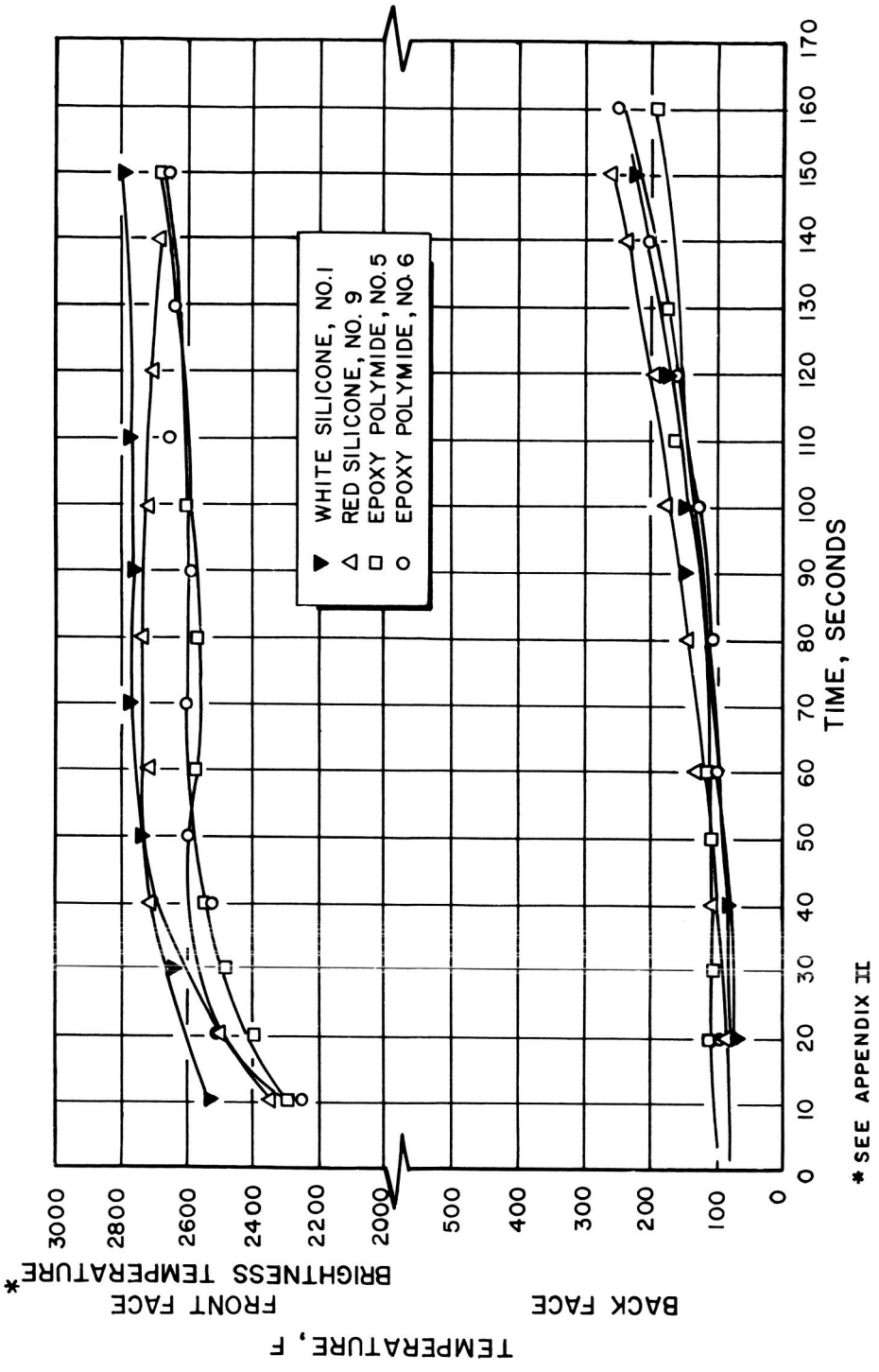

Figure 8. Natural Gas Oxygen Torch Test Constant 50 Btu/ft^2 sec Heat Flux Back-Face and Front-Face Temperatures vs Time

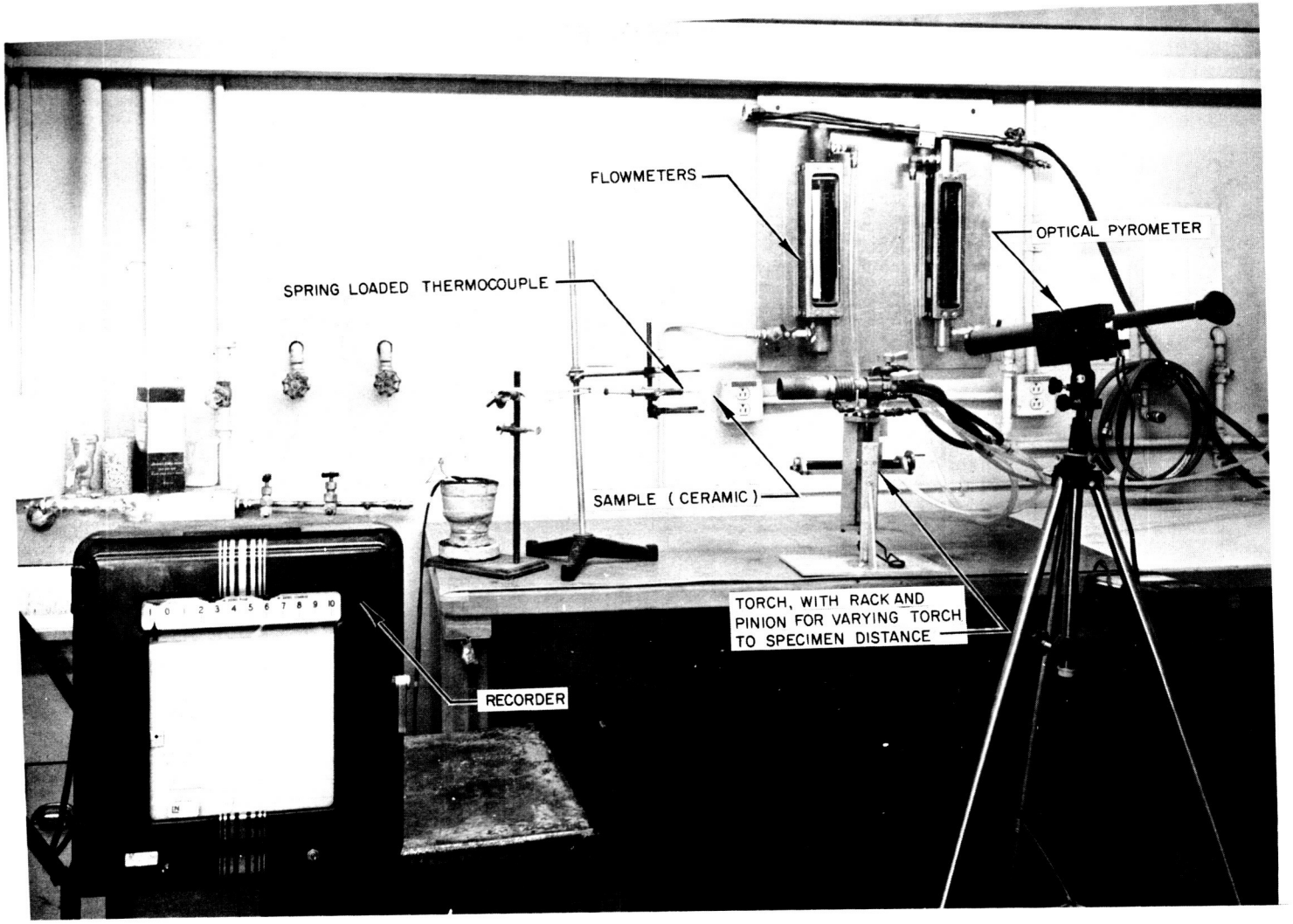

Figure 9. Natural Gas Oxygen Torch Test Variable Heat Flux Test Setup

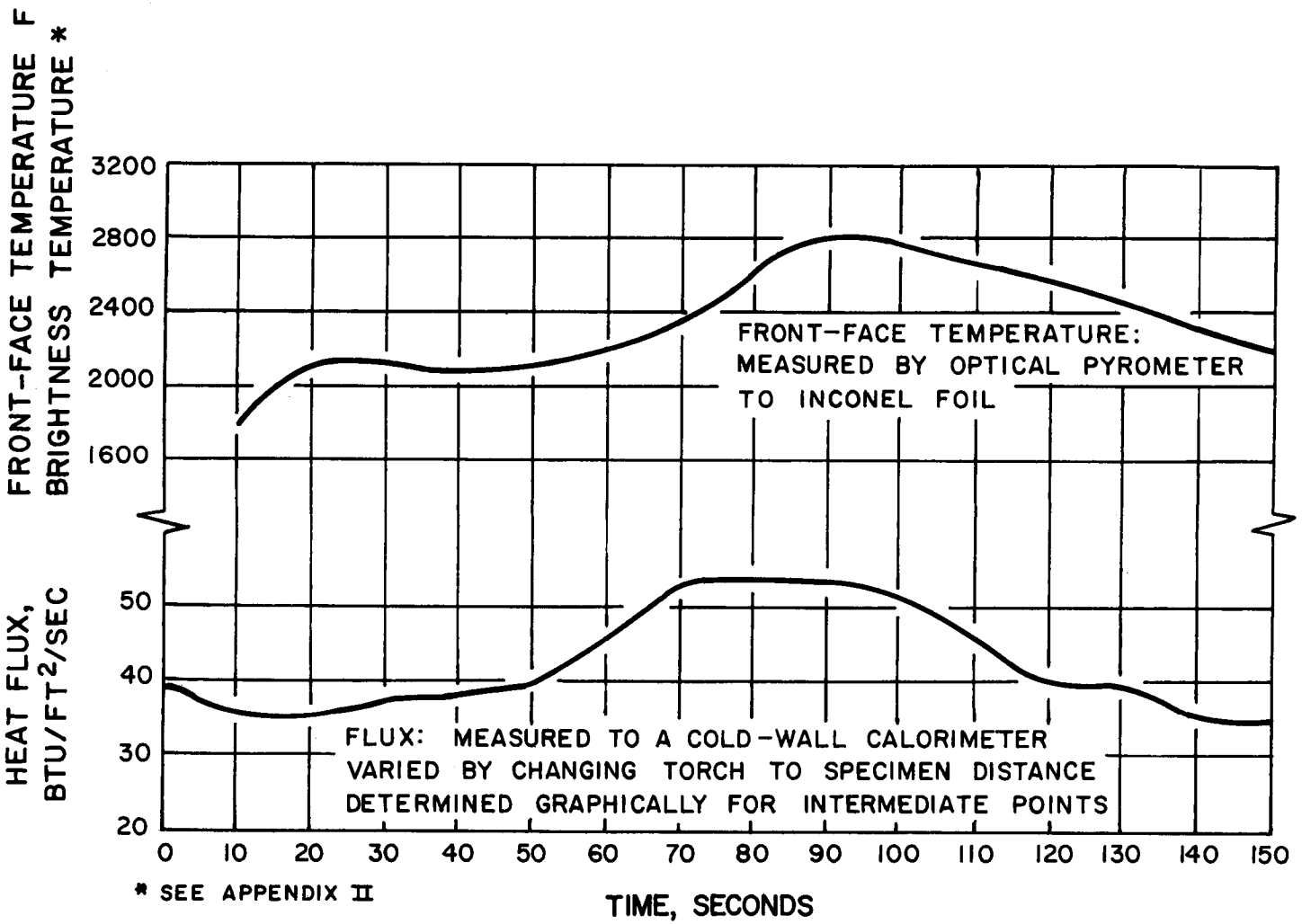

Figure 10. Natural Gas Oxygen Torch Test Variable Heat Flux, Heat Flux Range, and Front-Face Temperatures vs Time

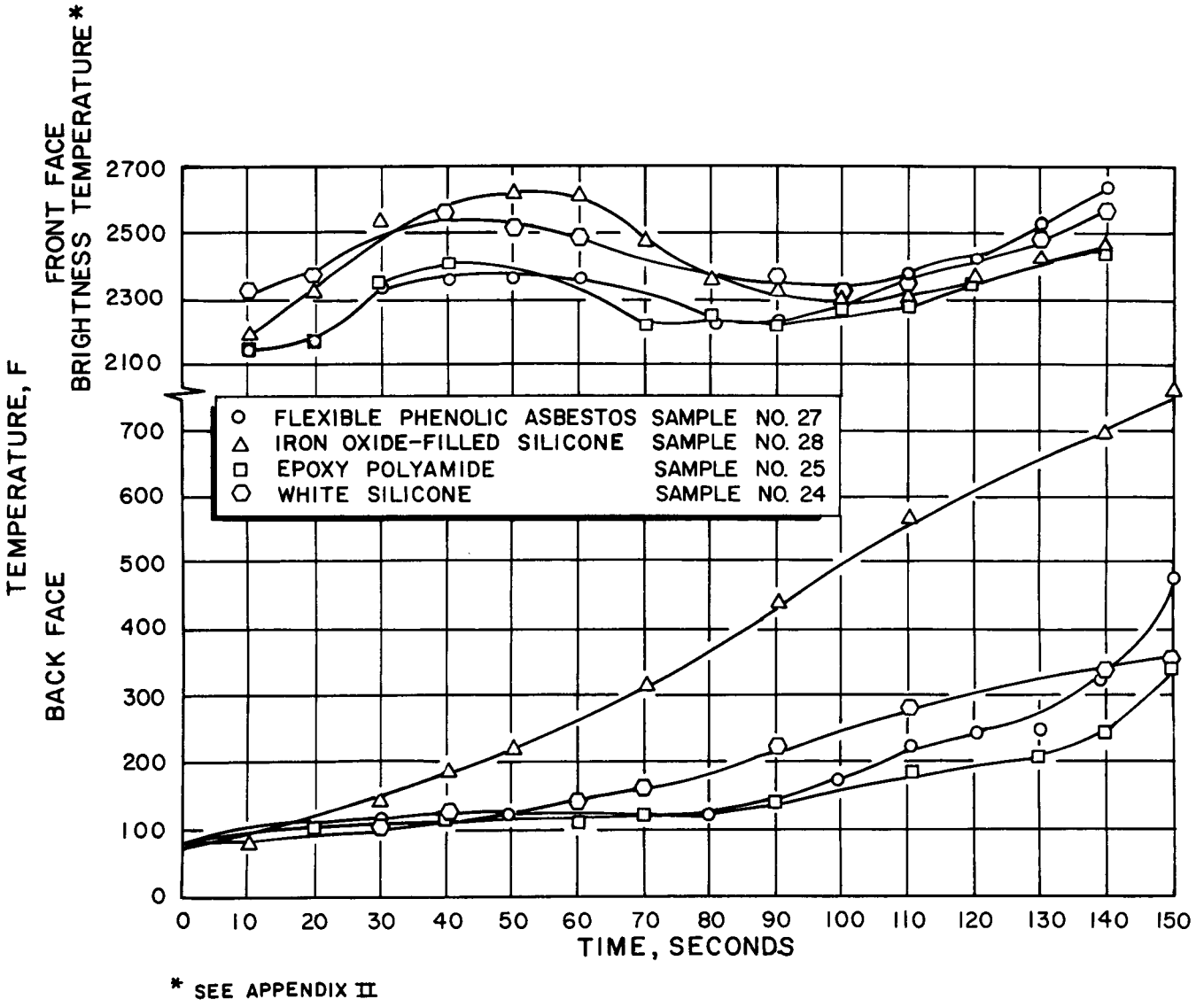

Figure 11. Natural Gas Oxygen Torch Test Variable Heat Flux Back-Face Temperatures and Front-Face Temperatures vs Time

The final method of testing these materials for thermal properties was to impose high radiant heat fluxes on them. The front-face temperature, intermediate temperature, and back-face temperature of a sample was measured while the sample was subjected to a radiant heat flux of 50 btu/ft^2/sec for 150 seconds or until failure. Fifty btu/ft^2/sec for 150 seconds was chosen as the test environment for comparison with the convective tests.

An oven composed of twenty-five 12-inch, 2000 watt, quartz-tube infra-red lamps, having a power density of 98 kilowatts per square foot when operating at a rated voltage of 240 V was used to provide the heat. Temperatures were monitored at the back face of the ablative material (ablative-aluminum plate interface) and internally half way between the front face and the back face by iron constantan thermocouples connected to a 150 F reference hot junction and a millivolt strip chart recorder. Front-face temperatures, for comparison, were determined by a platinum/platinum-13 percent rhodium thermocouple molded flush with the front surface of the material. Heat rates were determined by a 3-inch by 4-inch stainless steel plate (0.062 inch thick), coated with a lampblack-sodium silicate solution to increase absorbtivity.

Two specimens, mounted side by side in a fused quartz holding device (Fig. 12) with an insulating block between, were evaluated during each test. For some of the tests a motion picture camera was positioned to record the effects of the heat during the test duration. The specimens were a total of 0.250 inch thick when molded, including 0.062 inches of aluminum plate, and were 3- by 4-inch rectangles. The aluminum plate, used as a backup, was 2-1/2 by 3-1/2 inches to prevent radiation from reaching the panel around the sides of the specimen. Some samples were supplied by vendors as pre-molded sheets; these were adhesively bonded to the aluminum backup plate using a room temperature

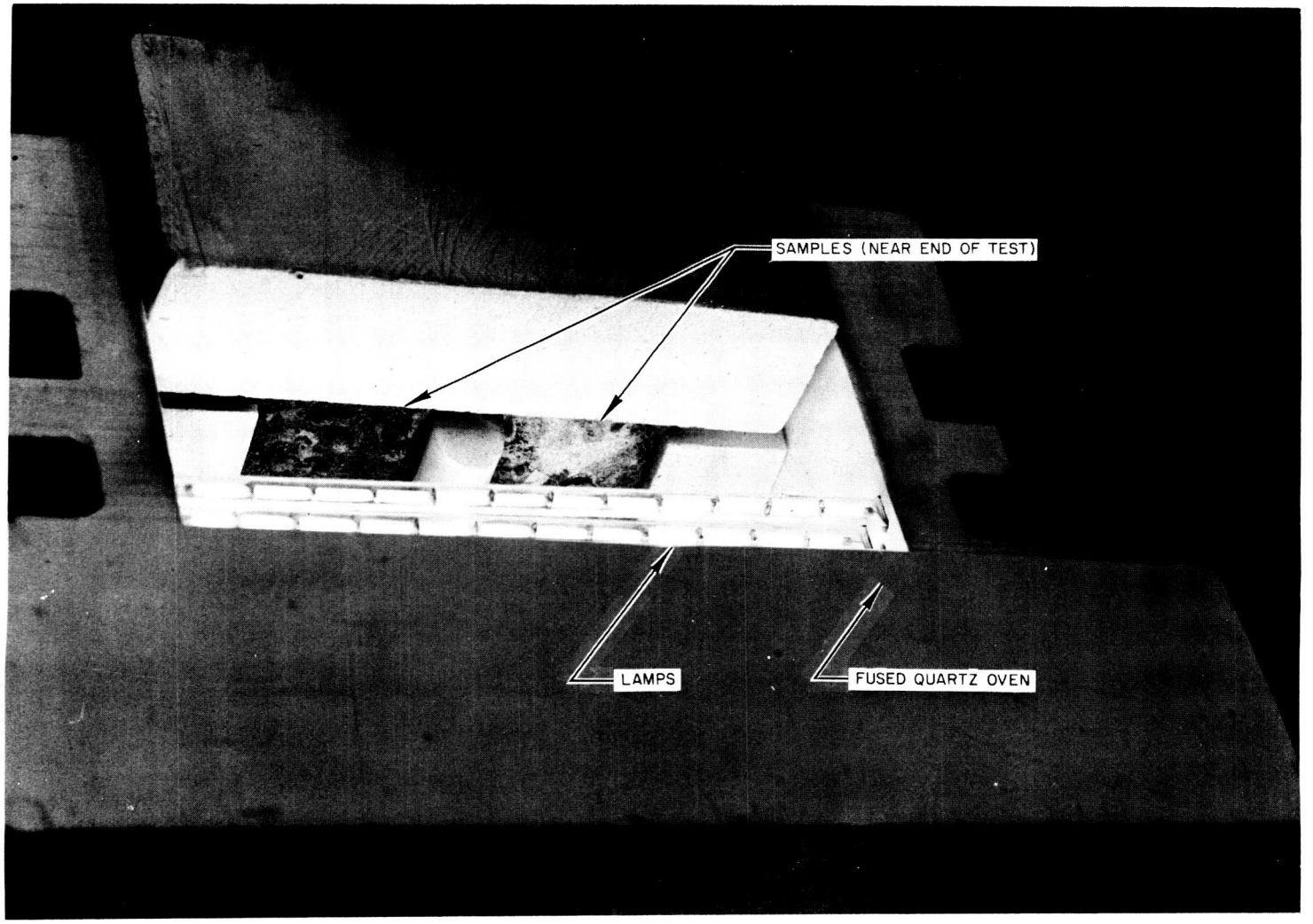

Figure 12. Test Setup for Radiant Heat Flux Tests

curing epoxy adhesive. During the tests a stream of air was passed over the quartz lamps for cooling. This air contributed to a slight convective heat load on the samples, but the velocity was of such a low value at the specimen faces that it was not measurable. Figure 13 shows the temperature rise with time of four samples tested under the radiant flux load.

The data resulting from the convective and radiative tests consisted of a recorder chart of the back-face temperature rise with time, a log of the front-face temperature with time and a determination of the weight change of the material. From these data a graphical representation of the back-face temperature rise with time was plotted, and the properties shown in Table II were determined. The effective heat of ablation, or heat blockage, H_{eff}, was calculated by the following equation:

$$H_{eff} = \frac{Q_o}{m_a} = \frac{\frac{q}{A} \cdot t}{\frac{m_a}{A}}$$

To assist in evaluation of the relative usefulness of the thermal insulations, a combination of parameters was selected which would rate these materials in terms of back-face temperature and total mass required to limit temperature rise of back face. This number, designated the "Performance Index," is a figure of merit, designed to show differences in materials not displayed by the effective heat of ablation. The equation used to reach this figure is:

$$P\ I = \frac{\frac{q}{A} \cdot t}{\frac{m_a}{A} \cdot T_f\ m_o} = \frac{H_{eff}}{T_f\ m_o}$$

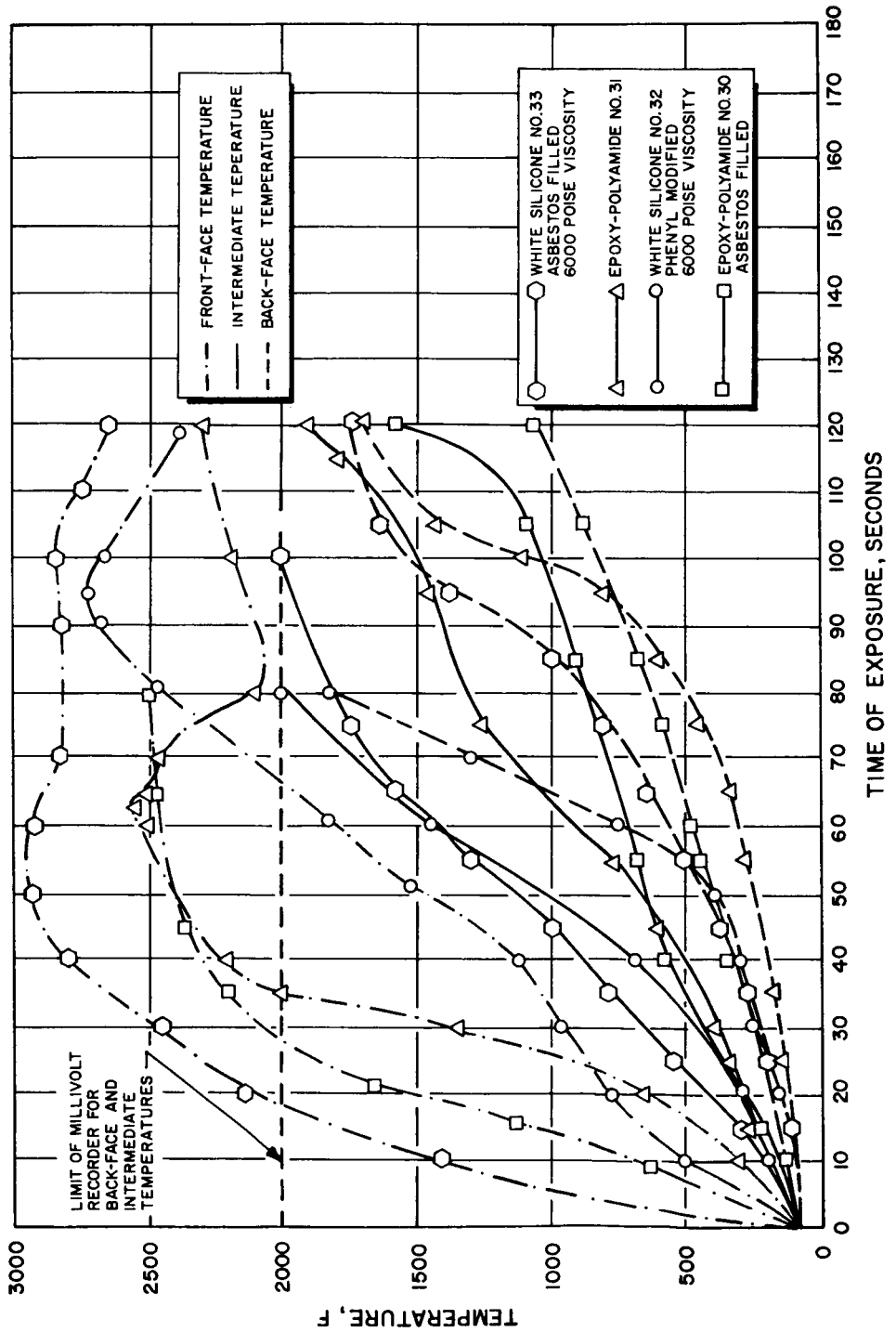

Figure 13. Radiant Heat Flux Tests, Back-Face and Front-Face Temperatures vs Time

The performance index is proportional to heat flux rate, and time, and is inversely proportional to the weight loss during ablation, the temperature at the back face of the specimen at the end of the test, and the initial mass of the specimen.

A suitable way of representing the ablative phenomenon is by the following equation: (4 and 5)

$$Q_{c\ +\ r} = Q_{rr} + Q_b + Q_p + Q_g + Q_k$$

Where:

$Q_{c\ +r}$ = total heat load, convective and radiative

Q_{rr} = heat reradiated from the char surface = $\epsilon\sigma\ Tw^4$

Q_b = heat absorbed by the "blocking effect" of gases

Q_p = heat absorbed in pyrolysis = $m_a\ H_p$

Q_g = heat absorbed by gas passage through the char layer = $\left[m_a\ \Gamma\ C_p\ (Tw = T_d)\right]$

Q_k = the heat conducted into the virgin plastic

It is desirable for an effective ablative to have a high value for Q_{rr}, Q_b, Q_p, Q_g, and to have a low value for Q_k. It has been postulated (5 and 9) that the factors of radiation from the surface char layer and the blocking effect may account for up to 70 percent of the heat of ablation. This fact seems to be reinforced when reference is made to Table II. The silicone resins, which, under these conditions of convective heat flux, form a luminous, highly emmittive char layer, show very high comparative values of H_{eff}. Also, during ablation of the highly iron oxide-filled silicones, a chemical reaction takes place at the surface of the char layer resulting in reduction of iron oxide to iron, (10). Further, silicones tend to expand toward the

flame, without benefit of addition of a specific intumescent agent, resulting in higher temperatures at the surface of the char. The performance of silicones in the variable heat flux test is enhanced because of a high surface temperature which increases reradiation and a higher heat flux, which most investigators (11 and 12) have found to increase effectiveness of ablators. A marked difference can be noted between the performance of the ablative composites in convective and radiant flux environments. This is apparently due to the loss of a great deal of the "blocking effect," Q_b which is presumed (5 and 9) to account for at least 20-30 percent of the incident flux reduction. The low molecular-weight degradation products, which issue as gases from the char layer, are somewhat transparent to the incident radiation.

A number of fillers were evaluated as possible means of upgrading the properties of the commercially available silicone and epoxy resins. Ammonium chloride which had been evaluated previously as a solid, (7), appeared to have the highest heat of ablation for high flux rate tests (1,400 - 5,000 btu/ft^2/sec.) when compared to tetrafluoroethylene, nylon, and two commercial plastic ablatives. It also performed adequately in further tests (8) as a filler for phenolic resins. When used in conjunction with silica fibers and potassium titanate or with aluminum oxide, silica fibers and "E" glass, i approximately doubled the effective heat of ablation of the base epoxy polyamide resin. When used in conjunction with potassium titanate it also had a relatively high performance index and exhibited a hard, tenacious char after thermal testing, a fact which had not been observed with unmodified and some proprietary epoxy polyamides, (Sample 5). The filled material

also reflects the fact of lower density with a performance index of over 3 times that of the unfilled resin. A substantial increase in H_{eff} is demonstrated by a titanium dioxide filled epoxy (Number 13, Table IIa) when compared to the unfilled material. There is, however, negligible improvement in the performance index, probably due to the higher density of the filled material. The differences in char structure of these two materials also helps to explain the differences in performance. The char formed on the titanium dioxide reinforced epoxy was fragil and very poorly held to the decomposing resin interface. A strong tightly held char as that obtained with the epoxy filled with ammonium chloride and potassium titanate, allowed the gases to percolate through the hot layer and decompose to their lowest molecular weight and their highest volume which in turn thickened the boundary layer. This tightly held char maintained a higher surface temperature and re-radiated a greater portion of the incident heat back into the surroundings.

The numerical figure of merit, performance index, although useful in evaluation of most of these materials, must be approached with care. Two of the materials (Sample 11 and 21, Table IIa), while not considered high performance ablatives, showed extremely high values for performance index in the constant convective heat flux test. It can be noted, however, that there was no virgin material left (the sample burned through) and consequently, the flame was not always impinging directly on ablative material. Also, the performance index is sensitive to the density of the test material, which in the case of the epoxy foam (Sample 11) is extremely low($36.3\ lb/ft^3$) further distorting the number already enlarged because of testing to complete removal of material.

If the value for the epoxy-silicone (Sample 21) is compared to the duplicate test run value (Sample 7) a marked difference will be observed. There are also wide differences in performance index evident in the variable convective heat flux tests. The room temperature curing silicone rubber, filled with iron oxide and chopped silica fibers (Samples 23 and 28), shows extremely high values of performance index when compared to the other materials. This anomaly is due primarily to the performance index's not being particularly sensitive to the back-face temperature, which in these two cases approaches and exceeds 800 F. It is obvious that if this material were used at this thin thickness (.125 inch) that adhesion to its substrate would have been lost much below 800 F. In these cases, however, the performance index is a more reasonable measure of performance than H_{eff}, which is quite distorted.

Each insulation system has its own particular limitations and disadvantages. It is quite possible the factors which enhance the performance of many of these ablative composites in the torch tests may also serve to reduce their effectiveness. If the intumescent, strong, and highly emittive char surface which appeared on most of the high performance silicone elastomers is not firmly bonded to the virgin material, the char may be lost in gross chunks by the action of vibration and high velocity gases. Also, most of these materials will burn, and it is probable that the gases issuing from them while they are ablating are highly flammable.

Of the various systems of insulation described, the foil-high silica fiber batting and the asbestos wire mesh composite are the only systems under active development. These two systems, as present tests determine, will be adequate in regard to temperature resistance, insulative ability, and gross weight addition to the flight vehicle. Neither these systems nor the ablative

or ceramic insulative systems, however, have been tested on a flight vehicle to the conditions expected on the Saturn V. If there is a need for an additional type of insulation after flight experience with the clustered F-1 is gained, Rocketdyne will be prepared to carry out advanced development tests, such as wind tunnel and vibration tests.

ACKNOWLEDGEMENT

I wish to express my appreciation to the following person whose contributions of time and energy made this publication possible. Mr. Robert Mowers, who proofread, consulted and carried out many operations which otherwise could not have been accomplished.

APPENDIX I

Explanation of Symbols

A = frontal area of the specimen, ft^2
the frontal area of all convectively tested specimens was the same, $2.18 \times 10^{-2} ft^2$, the radiant heat flux test specimens had an area of $8.33 \times 10^{-2} ft^2$

Cp = specific heat of gas Btu/lb F

H_{eff} = heat blockage, Btu/lb

H_p = heat of pyrolysis, Btu/lb

$\frac{q}{A}$ = heat flux rate $Btu/ft^2/sec$

$\frac{Qo}{A}$ = total heat flux Btu/ft^2

m_a = weight of ablated material

m_o = original weight, lbs

t = time, seconds

T_d = decomposition temperature, F

T_f = final temperature at end of test R

T_w = wall temperature (char surface)

Greek Letters

Γ mass fraction of solid converted to gas

ϵ emissivity

σ Stefan-Boltzmann constant

or ceramic insulative systems, however, have been tested on a flight vehicle to the conditions expected on the Saturn V. If there is a need for an additional type of insulation after flight experience with the clustered F-1 is gained, Rocketdyne will be prepared to carry out advanced development tests, such as wind tunnel and vibration tests.

ACKNOWLEDGEMENT

I wish to express my appreciation to the following person whose contributions of time and energy made this publication possible. Mr. Robert Mowers, who proofread, consulted and carried out many operations which otherwise could not have been accomplished.

APPENDIX I

Explanation of Symbols

A = frontal area of the specimen, ft^2
the frontal area of all convectively tested specimens was the same, $2.18 \times 10^{-2} ft^2$, the radiant heat flux test specimens had an area of $8.33 \times 10^{-2} ft^2$

Cp = specific heat of gas Btu/lb F

H_{eff} = heat blockage, Btu/lb

H_p = heat of pyrolysis, Btu/lb

$\frac{q}{A}$ = heat flux rate $Btu/ft^2/sec$

$\frac{Qo}{A}$ = total heat flux Btu/ft^2

m_a = weight of ablated material

m_o = original weight, lbs

t = time, seconds

T_d = decomposition temperature, F

T_f = final temperature at end of test R

T_w = wall temperature (char surface)

Greek Letters

Γ mass fraction of solid converted to gas

ϵ emissivity

σ Stefan-Boltzmann constant

APPENDIX II

The front-face temperature or "brightness temperature," as graphically portrayed on Figs. 8, 10, 12, and 13, are the temperatures as measured by an optical pyrometer and not the true temperature at the surface. Investigators have attempted to estimate the true surface temperature by measuring the surface brightness temperature of the material and assuming a value for emissivity (6 and 13), a method which admittedly is inadequate. The emissivity value assumed has ranged from 0.4 to 0.8, but, because of the possibility of widely differing surface temperatures, depending upon the emissivity of the charring material, the surface brightness temperature is recorded as the surface temperature.

REFERENCES

1. Rocketdyne Internal Correspondence, D. Trujillo, originator
2. Rocketdyne Internal Correspondence, J. Brukiewa, originator
3. Rocketdyne Internal Correspondence, D. Calkins, originator
4. Steurer, Wolfgang H., "Principles and Capabilities of Ablation" Paper presented at ASTM National Meeting, San Francisco, California October 10-16, 1959
5. Reinikka, E. Arnold and Wells, Philip B., "Charring Ablators in Lifting Re-Entry" Paper presented at AIAA Summer Meeting, Los Angeles, California, June 17-29, 1963
6. Vojvodich, Nick S., and Winkler, Ernest L., "The Influence of Heating Rate and Test Stream Oxygen Content on the Insulation Efficiency of Charring Materials" Technical Note D-1889, National Aeronautics and Space Administration, July, 1963
7. Chapman, Andrew J., "An Experimental Investigation of Several Ablation Materials in an Electric-Arc-Heated Air Jet," Technical Note D-1520, National Aeronautics and Space Administration, April, 1963
8. Chapman, Andrew J., "An Experimental Evaluation of Three Types of Thermal Protection Materials at Moderate Heating Rates and High Total Heat Loads," Technical Note D-1814, National Aeronautics and Space Administration, July, 1963
9. Brooks, William A. Jr., Swann, Robert T., and Wadlin, Kenneth L., "Thermal Protection for Spacecraft Entering at Escape Velocity," Paper #513 F, presented at Society of Automotive Engineers, National Aeronautics meeting, New York, April 3-6, 1962

10. Farber, E. L., "The Development of Polymeric Coatings for Rocket Nozzle Cooling," Member's Report to the National Aeronautics and Space Administration, Research Advisory Committee on Materials, September, 1962

11. Peters, Roger W. and Wilson, R. Gale, "Experimental Investigations of Convective and Radiative Heat Loads on the Performance of Subliming and Charring Ablators," Technical Note D-1355, National Aeronautics and Space Administration, July, 1962

12. Mixer, R. Y. and C. W. Marynowski, "A Study of the Mechanism of Ablation of Reinforced Plastics," Wright Air Development Division, WADC Technical Report 59-668, Part 1, February, 1960

13. Burhard, K., Hoercher, W., et al, "Characterization of Carbonized Plastic Composites in Hyperthermal Environments," Technical Documentary Report No. ASD TDR-62-746 Directorate of Materials and Processes, Aeronautical Systems Division, Air Force Systems Command, Wright Patterson Air Force Base, Ohio, August 1962

TABLE 1

A COMPARISON OF THREE TYPES OF INSULATION SYSTEMS*

	Epoxy	Ceramic	Foil and Batting
Density, lb/ft^2 at necessary thickness	Polyamide No. 6 1.83 lb/ft^2 at 1/4-in. thick	M 31 (3/8 in. thick) 1.97 lb/ft^2	0.53 lb/ft^2
Estimated Cost/ft^2 raw material plus Fabrication	11.5 12.5	5.00 - 5.50 ~ 10.00	2.00 - 3.00 ~ 6.00
Fabrication Ease	Paint on or spray	Must be premolded and attached by mechanical fasteners	Must be performed to accommodate various contours and attached by fasteners
Repairability	Good	Can be trowelled	Remove section and weld
Useable Upper Temperature	Unlimited	1750 (10 percent shrinkage)	2000
Water Absorption	1 percent	76 percent	100-350 percent
Impact Strength		4.5 in. lbs.	----
Tensile Strength	480 psi		----
Flexural Strength	Flexible	720 $lbs/in.^2$	----
Vibration Resistance	Good	Poor	Good

*There are some advantages of ablative cooling which cannot be tabulated. A given amount of material to maintain a given back-face temperature will take up much less space than either of the three other systems. This is because the ablative material will be painted or trowelled directly on to the substrate, without benefit of supporting brackets. Also, since fabrication and application occur simultaneously, there is no tooling required. Finally, the weight of ablatives decreases during flight time, thereby adding a certain amount of net payload that the vehicle can carry.

TABLE IIa

TABULATED RESULTS OF CONSTANT 50 BTU/ft^2 SEC CONVECTIVE HEAT FLUX TESTS

Specimen No.	Sample Descriptions (Base Resin and Fillers)	Initial Weight m_o Lbx10^{-2}	Weight Loss m_a Lbx10^{-2}	Weight Loss $\frac{m_a}{A}$ Lb/ft^2	Thickness Initial Inches	Thickness Final Inches	Final Virgin Material Inches	Density Lb/ft^3	Length of Test Seconds	Total Heat $\frac{Q_o}{A}$ Btu/ft^2	Heat Blockage H_{eff} Btu/lb	Temperature at End of Test T_F, ^oR	Performance Index $\frac{H_{eff}}{T_F, m_o}$
1	Room Temperature Curing Silicone, White, 200 Poise Viscosity	4.06	0.69	0.31	0.295	0.311	0.095	68.7	115	5,750	18,196	678	661
2	Room Temperature Curing Silicone, White, 6,000 Poise Viscosity	4.66	1.09	0.49	0.300	0.515	0.100	84.9	150	7,500	15,030	587	549
3	Epoxy Silicone Polyamide, Cork Filled	2.91	1.77	0.81	0.313	0.205	None	52.0	130	6,500	8,020	579	445
4	Buna-N Phenolic, Inorganic Subliming Salt Filler	7.70	2.78	1.2	0.501	0.509	0.288	85.5	300	15,000	11,810	661	232
5	Epoxy Polyamide, Ammonium Chloride, Potassium Titanate, Silica Fibers, as Fillers	3.95	2.88	1.3	0.317	0.278	0.065	68.6	170	8,500	6,440	733	222
6	Epoxy Polyamide, Unknown Filler	4.88	2.12	0.97	0.327	0.388	0.117	81.7	200	10,000	10,288	680	310
7	Epoxy Silicone Polyamide, Phenolic Microballoons Filler	3.49	1.94	0.88	0.309	0.000	0.000	67.4	130	6,500	7,390	685	332
8	Epoxy Polyamide, Ammonium Chloride Silica Spheres, Phenolic Microballoons as Fillers	3.23	3.23	1.48	0.312	0.000	0.000	54.9	130	6,500	4,390	735	184
9	Room Temperature Curing Silicone, Iron Oxide Filled, Chopped Silica Fibers	5.19	0.93	0.42	0.305	0.522	0.139	93.6	130	6,500	15,260	714	411
10	Epoxy Casting Resin (Unfilled Research Resin)	6.80	2.66	1.21	0.505	0.292	0.292	74.4	60	3,000	1,278	563	33
11	Epoxy Foam (Unknown Filler)	1.47	0.69	0.32	0.500	--	--	36.3	50	2,500	7,812	560	949

TABLE IIa

(Continued)

Specimen No.	Sample Descriptions (Base Resin and Fillers)	Initial Weight m_o Lbx10^{-2}	Weight Loss m_a Lbx10^{-2}	Weight Loss $\frac{m_a}{A}$ Lb/ft^2	Thickness Initial Inches	Thickness Final Inches	Final Virgin Material Inches	Density Lb/ft^3	Length of Test Seconds	Total Heat Load $\frac{Q_o}{A}$ Btu/ft^2	Heat Blockage H_{eff} Btu/lb	Temperature at End of Test T_F, ^oR	Performance Index $\frac{H_{eff}}{T_F, m_o}$
12	Epoxy Polyamide, Silica Fibers, Titanium Dioxide Fillers	3.86	1.94	0.89	0.375	0.000	0.000	57.0	90	4,500	2,319	620	96
13	Epoxy Polyamide Titanium Dioxide Filler	7.11	4.34	1.98	0.500	--	--	78.6	150	7,500	3,787	650	82
14	Epoxy Polyamide, No Filler	6.45	4.82	2.21	0.500	--	---	71.2	120	6,000	2,714	668	63
15	Epoxy Polyamide, Ammonium Chloride, Silica and "E" Glass Fibers as Fillers	4.06	2.94	1.34	0.410	0.279	0.10	54.6	83	4,150	3.097	575	132
16	Same as Number 5	4.82	2.13	0.97	0.428	0.370	0.18	68.6	120	6,000	6,185	600	213
17	Epoxy Polyamide Ammonium Chloride, Aluminum Oxide Silica and "E" Glass Fibers as Fillers	5.57	2.61	1.19	0.520	0.406	0.26	59.2	147	7,350	6,176	615	180
18	Polyurethane Rubber 15% Potassium Titanate Filled	3.07	1.90	0.87	0.230	0.090	0.000	70.0	60	3,000	3,444	620	181
19	Polyurethane Rubber 40% Silica Fibers as Filler	3.54	1.12	0.51	0.239	0.137	0.10	79.0	80	4,000	7,797	775	284
20	Same as Number 3	2.26	1.77	0.81	0.266	0.050	0.02	67.4	50	2,500	3,082	590	231
21	Same as Number 7	2.00	0.78	0.35	0.254	Burned Through	0.00	52.0	75	3,750	10,714	610	878
22	Phenolic Bonded Cork	2.96	2.73	1.25	0.499	0.000	0.00	32.9	65	3,250	2,600	767	114

TABLE IIb

TABULATED RESULTS OF VARIABLE CONVECTIVE HEAT FLUX TESTS

Specimen No.	(Base Resin and Fillers)	Initial Weight m_o Lbx10^{-2}	Weight Loss m_a Lbx10^{-2}	Weight Loss $\frac{m_a}{A}$ Lb/ft^2	Thickness Initial Inches	Thickness Final Inches	Final Virgin Material Inches	Density Lb/ft^3	Length of Test Seconds	Total Heat Load $\frac{Q_o}{A}$ Btu/ft^2	Heat Blockage H_{eff} Btu/lb	Temperature at End of Test T_F, ^oR	Performance Index $\frac{H_{eff}}{T_F, m_o}$
23	Same as Number 9	1.96	0.53	0.24	0.110	0.25	0.0	93.6	150	6,110	25,458	1,155	1,249
24	Room Temperature Curing Silicone Rubber, White, Asbestos Filled 6,000 Poise Viscosity	2.71	0.39	0.17	0.250	0.42	0.100	62.0	150	6,110	15,660	820	704
25	Same as Number 5	3.87	1.95	0.89	0.314	--	--	68.6	150	6,110	6,865	800	221
26	Flexible Phenolic Asbestos	4.15	2.14	0.98	0.250	0.30	--	75.0	128	5,220	5,310	610	191
27	Same as Number 26	3.93	2.41	1.10	0.250	--	--	75.0	150	6,110	5,550	940	165
28	Same as Number 9	2.03	0.47	0.21	0.125	0.25	0.0	93.6	150	6,110	29,095	1,220	1,175
29	Same as Number 11	0.81	0.34	0.15	0.250	Burned Through	--	36.0	20	721	890	985	136

TABLE IIc

TABULATED RESULTS; RADIANT HEAT FLUX TESTS; 50 Btu/ft^2-SEC

Specimen No.	Sample Description (Base Resin and Filler)	Initial Weight m_o $Lbx10^{-2}$	Weight Loss m_a $Lbx10^{-2}$	Weight Loss $\frac{m_a}{A}$ Lb/ft^2	Thickness Initial Inches	Thickness Final Inches	Final Virgin Material Inches	Density Lb/ft^3	Length of Test Seconds	Total Heat $\frac{Load\ Qo}{A}$ Btu/ft^2	Heat Blockage H_{eff} Btu/lb	Temperature at End of Test T_F, °R	Performance Index $\frac{H_{eff}}{T_F,\ m_o}$
30	Epoxy Polyamide With Titanium Dioxide Filler	15.2	8.15	0.978	0.188	0.20	0	92	120	6,000	6,130	1,535	26.2
31	Epoxy Polyamide Same as Number 6	13.0	5.60	0.672	0.188	0.40	0	81.7	120	6,000	8,928	2,160	31.7
32	Room Temperature Curing Silicone, Same as Number 2	11.8	11.8	1.41	0.188	0	0	84.9	120	6,000	4,255	3,210*	11.2
33	Room Temperature Curing Silicone, Same as Number 24	8.73	2.23	0.267	0.188	0.3	0	62	120	6,000	22,471	2,060	12.4
34	Buna-N Phenolic, Same as Number 4	7.4	5.68	0.681	0.125	0.1	0.05	85.5	70	3,500	5,139	1,235	56.2
35	Epoxy Silicone Polyamide Same as Number 3	5.75	4.41	0.592	0.188	0.2	0	52.0	70	3,500	5,912	2,460*	41.8
36	Epoxy Polyamide, Same as Number 5	10.1	8.18	0.981	0.188	0.3	0	68.6	67	3,350	3,414	1,360*	24.8
37	Epoxy Polyamide, Same as Number 8	7.8	6.81	0.817	0.188	0	0	54.9	67	3,350	4,100	1,160	45.3
38	Room Temperature Curing Silicone, Same as Number 9	12.3	3.15	0.378	0.188	0.3	0.2	93.6	89	4,450	11,770	1,210	79.0
39	Room Temperature Curing Silicone, Same as Number 1	9.87	5.07	0.608	0.188	0.40	0	68.7	89	4,450	7,319	1,535	48.3
40	Phenolic Bonded Cork,	2.38	2.38	0.285	0.125	0	0	32.9	94	4,700	+	2,460*	+

+Unable to calculate, sample had burned completely through and some of the aluminum backing plate had melted.

*The temperatures marked were not directly obtainable. In some instances, the backface temperature wildly oscillated or exceeded the capacity of the recorder. These temperatures were estimated by extrapolation or interpolation of the temperature curves.